



## Comparison between Numerical Results and the Lab Results in Analyzing the Buckling Behavior of Plates Optimized by Longitude Stiffeners

Loghman Rahemi<sup>1</sup>, Abolfazl Shamsai<sup>2</sup>, Kamal Rahmani\*<sup>1</sup>, Saber Peroti<sup>1</sup>

<sup>1</sup>Department of Civil Engineering, Mahabad Branch, Islamic Azad University, Mahabad, Iran

<sup>2</sup>Department of Civil Engineering, Sharif University of Technology, Tehran, Iran

### ABSTRACT

This research expresses the non-linear analysis of the impacts of the cross sections and number of stiffeners in improving the buckling and ultra-buckling behavior of plates that have been stiffened with longitude stiffeners under the impact of pressure axial load and prior to final destruction with the parameters free from stress dimensions as imposed to the materials submission stress ( $\frac{\sigma_{uF}}{\sigma_y}$ ) and deformation of the end part of sample to the initial length of the sample ( $\frac{\delta_{end}}{\delta_{int}}$ ). The results obtained from the numerical analysis were then compared to the lab results and the accuracy was measured. The numerical analysis of samples was performed by using ABAQUS software. According to the results, it could be stated that as the number of stiffeners increases in general status of dimensionless parameter ( $\frac{\delta_{end}}{\delta_{int}}$ ) decreases in numerical analysis, and subsequently the dimensionless parameters ( $\frac{\sigma_{uF}}{\sigma_y}$ ) of the samples increases. In fact, the impact of number of stiffeners could be expressed as increase in the resistance and decrease in deformation in the samples; however, the impact of cross sections of stiffeners in longitudinal deformation of each group of samples could be described as, the model with T-shape stiffener has the least longitudinal deformation and the model with R-shape stiffeners has the highest longitudinal deformation. The final resistance of buckling in models starts from approximately 40 percent of submission resistance and increases up to 70 percent of submission resistance in samples. In this research, the lab data performed on steel plates with longitude stiffeners were used with three T, L and R cross sections types to compare and check the accuracy of results of numerical analysis. The numerical analysis results showed a difference of approximately 5 percent with the lab results; the highest difference to be on deformation and initial welding. The method used in analysis could study the results in both elastic and plastic regions.

**Key words:** Optimized plate, stiffeners, pressure axial loads, buckling behavior, ultra buckling behavior.

### INTRODUCTION

The main structure members in offshore off-coastal structures are the box girders, load bearing plates, bridges and plates optimized by stiffeners. The pressure axial load is one of the most essential loads imposed on the optimized plates that cause the plates bend in length. An example of this type of distortion has been shown in figure (2) [1,2].

Stiffened structures are efficient structures because by using and increasing stiffeners, the load bearing power and resistance of this type of structures increase. Although the mechanism of destruction of stiffened plates under the impact of pressure load is a complicated engineering issue that is caused by a combination of several factors such as geometry of the plate and stiffeners, their materials, border conditions and loading, in order to analyze this type of structure elements in Orthotropic plates theory, we predicted the buckling stress as to be all across [3]. The

geometric imperfection caused by manufacturing is inevitable in stiffened plate. The mechanism of stiffened plates buckling depends on the hardness of members in line with initial bending and happens with respect to the hardness of bending members in the plates or stiffeners [4,5]. In this study the impact of the cross sections and number of stiffeners in improving the buckling behavior of plates is examined in numerical and comparison is made with the lab results and the accuracy is measured.

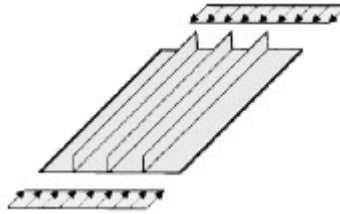


(Figure1): Plates optimized with stiffeners under impact of axial load

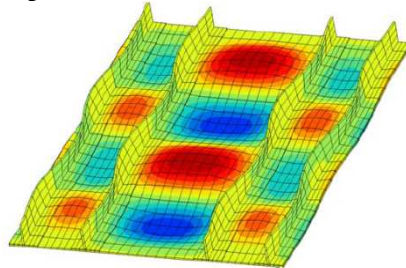


(Figure2): Deformation of optimized plate under impact of axial load

**Definition of problem (Research Question):**

Since this research is performed in limited element form and with an innovative method; and on the other hand, due to the lack of sufficient facilities to perform lab researches, it was decided to use the lab results performed for measuring the accuracy of this innovative method. For this purpose, among several existing lab researches, a series of very good lab information on the impact of cross section of longitude stiffeners on the buckling behavior of steel plates exposed to pressure axial load was chosen that had already studied and the impacts of buckling and ultra-buckling capacity prior to final rupture.

The numerical analysis method which has been employed is based on the following hypotheses:

1. The cross section of plate stays with no deformations after bending.
2. The cross section of the middle opening stays elastic.
3. The proportion of the initial deformation to the secondary deformation is the plastic joint.
4. The height of stiffeners fixed on plates by using the relations related to the orthotropic plates theory is adjusted in a way that the general and local buckling modes match.

**Definition of geometry of samples**

Sixteen samples of overall plates with the same dimensions and physical specifications are classified in six groups as listed in tables (1 and 2).

The geometric dimensions of the plate are as follows:

length: 650mm, width: 325mm and thickness: 4.8mm, as staying the same for all models.

This data has been presented by Mr. Ghosh to study the impacts of cross section and number of R, L and T type stiffeners on the buckling behavior of stiffened plates [6].

**Table 1: Introducing analysis samples**

Modeling classes	Plates stiffened with stiffeners	Samples labeling
1	Plate without stiffeners	MO
2	Plate with one longitudinal stiffener	MRI-ML-1-MT1
3	Plate with two longitudinal stiffeners	MR2-MI-2-MT2
4	Plate with three longitudinal stiffeners	MR3-MI-3-MT3
5	Plate with four longitudinal stiffeners	MR4-MI-4-MT4
6	Plate with five longitudinal stiffeners	MR5-MI-5-MT5

The plates have been optimized by three stiffeners in different cross sections.

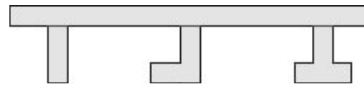


**(Figure3): Plate optimized with three longitudinal stiffeners.**

An example of an optimized plate that is made by combining the plate with stiffener T has been shown in figure (4).

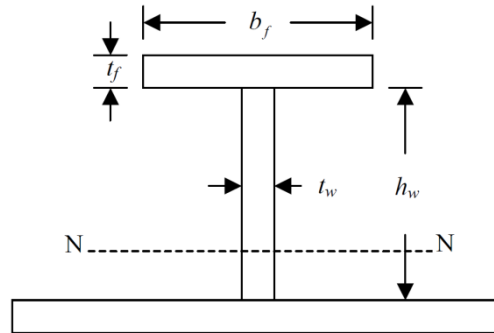


**(Figure4): Plate optimized with (T) shape stiffener.**

The geometric specifications of the stiffeners are listed in table(2). The limited element models are simulated based on the specifications of these samples and are analyzed accordingly.

**Table2: Introduction to the geometric specifications of stiffeners (in mm)**

Cross section of stiffeners	Tw	Hw	Tr	br
Rectangular shape ( R)	8	35	-	-
L-shape	7.5	35	4	20
T-shape	7.5	35	6	26

**Modeling in limited element software**

The analysis of samples was performed by using ABAQUS limited element software [4]. Analysis of non-linear buckling was performed by using Riks method. This method is useful for presenting a longitudinal buckling mode and changing large non-linear deformations as well as presenting the detailed results. In the analysis, the 4-knot shell elements (S4 and S4R) were used, among their properties, one may note limited rotations and the property of its membrane tension. Each element knot has six degrees of freedom. This element has the capability of being used in elastic and plastic regions with the stiffening strains or softening strains. Figure (5) shows this type of element.

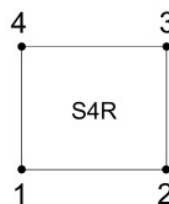


**(Figure5): Elements used in samples meshing**

*Border conditions in models analysis*

Optimized meshing in stiffened plates seems necessary to achieve sufficient precision in assessing the stressing behavior and plastic fracture as well as integrity of results of limited analysis and lab results. The trial and error method was used for proper control of elements. That is, the elements were made smaller and the results were compared with the initial mesh result. The process was repeated in sufficient frequency to obtain suitable size of elements. It should be noted that the number of longitudinal meshes of models does not have much impacts in amount of buckling value of samples; however, width meshing has extraordinary impacts because when modeling was done with larger meshes to reduce models analysis time, we noticed large errors in the numerical results than lab results; therefore, this problem was removed by increasing in number of width elements. In addition, in simulation of lab samples, the border conditions of supports have been considered plain.

*Geometric imperfections of models*

In the analysis of non-elastic buckling the answer lies in continuation bifurcation section where knowing the initial geometric imperfections of stiffener and plain are very important in the issue, and it is done by using Imperfection-Option parameters in ABAQUS limited element software. The imperfection models are obtained from analyzing special values of general buckling modes. Deformation of the selected mode for a full opening is an ascending semi-wave; however, it is descending semi-wave for a half opening. No special simulation has been performed for the stress of welding residue in this study. The axial pressure is imposed on the simulated elements of plate homogenously and the model is then analyzed. This analysis makes some errors and mistakes in the amount of maximum deformation calculation as its amount (degree of error) has been already measured. This process could be applied in simulating the process of welding residue stress and the initial geometric imperfection. Those stresses have been imposed in framework of initial deformations in the “Ghosh” samples and are almost in accordance with the presented model [6]. In this process, first, the buckling analysis is performed by ABAQUS and in rapture behavior by using ABAQUS. The corrected Riks method, which was performed by ABAQUS software, is based on this assumption that loading is relative. That is, the size and magnitude of the load only change by Scalar parameters. The nature of this method is that the only balance path in space could be drawn by knot variables and loading parameters as well as simultaneous solving of displacements and loadings. The base algorithm is used by using Newton Method only for 1% increase in strain through extrapolation. This method is workable even for unstable and complicated structures as well [7].

*Materials specifications*

The specifications of steel consumed by Ghosh have been introduced to the software in stiffening stress-strain diagram. The stiffening strain has important impacts on the behavior of non-linear buckling of plates. In this research, the behavior of subject materials has been modeled both for the plain and stiffener in the elastic and plastic modes with E/65 stiffening strain factor, as shown in figure 6. The Poission Coefficient in the FEM tests and calculations has been taken as 0.3.

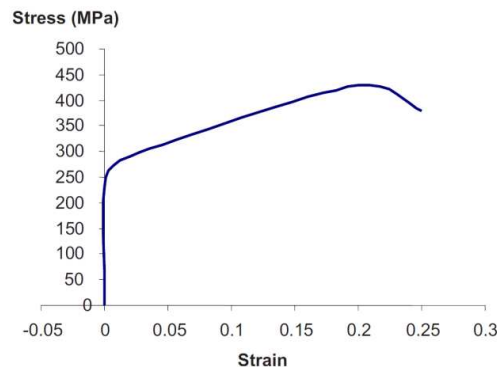


(Figure 6): Stress-strain curve for materials

**Buckling stress of plates**

In each test, the amount of stress imposed could be calculated by dividing the final load on general cross section of plates and stiffeners, as shown in equation (1):

$$\sigma_u = P_u / (A_p + A_s) \tag{1}$$

In which:

- $\sigma_u$ : The stress of imposed destruction
- $A_p$ : Cross section of the plate
- $P_u$ : Final load
- $A_s$ : Stiffener cross section

next stage; three buckling waves are added to the sample deformation. A non-linear Riks analysis is then performed to calculate final rapture stress and post The crippling load could be calculated by summing the multiplication product of the plate submission stress multiplied in the plate area with the stiffeners submission stress in their area; it is equal to equation (2):

$$P_q = \sigma_{yp} \cdot A_p + \sigma_{ys} \cdot A_s \tag{2}$$

- $\sigma_{yp}$ : Plate submission stress
- $\sigma_{ys}$ : Stiffener submission stress

$P_q$ : Crippling load

The results have been presented in table number(3) in form of dimensionless parameter that shows the ratio of final submission stress obtained from results of analysis(σult,FEA) to the final submission stress obtained from lab results (σult,Exp) of Mr. Ghosh and the dimensionless parameter to the final submission stress from the analysis results (σult,FEA) to the plate materials and stiffener submission stresses (σy) and the dimensionless parameter to the maximum deformation at the end of sheet plate ( $\delta_{end}$ ) to the initial length of sheet plate ( $\delta_{int}$ ) as shown in table( 3).

**Table3: Comparison between numerical and lab results of models**

Row	Models	$\frac{\sigma_{uF}}{\sigma_{uE}}$	$\frac{\sigma_{uF}}{\sigma_y}$	$\frac{\delta_{end}}{\delta_{int}}$
1	M0	1.001	0.40	0.0019
2	MR1	1.028	0.48	0.0017
3	ML1	1.017	0.52	0.0015
4	MT1	1.010	0.54	0.0017
5	MR2	1.006	0.58	0.0017
6	ML2	1.029	0.60	0.0013
7	MT2	1.022	0.59	0.0012
8	MR3	1.024	0.61	0.0011
9	ML3	1.042	0.60	0.0012
10	MT3	1.036	0.63	0.0012
11	MR4	1.031	0.65	0.0010
12	ML4	1.046	0.62	0.0011
13	MT4	1.029	0.67	0.0010
14	MR5	0.976	0.69	0.0011
15	ML5	0.983	0.67	0.0009
16	MT5	0.974	0.70	0.0010

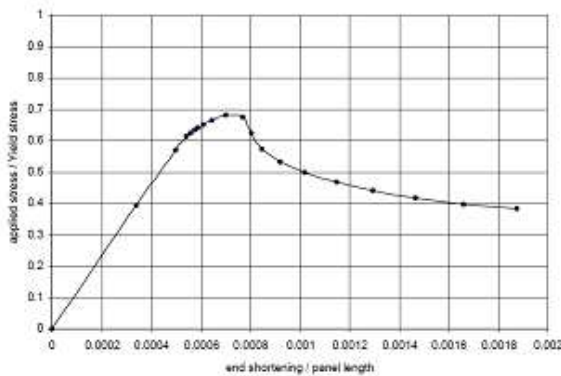


(Figure 7): Curve of changes of ( $\frac{\delta_{end}}{\delta_{int}} - \frac{\sigma_{uF}}{\sigma_y}$ ) of M0 sample

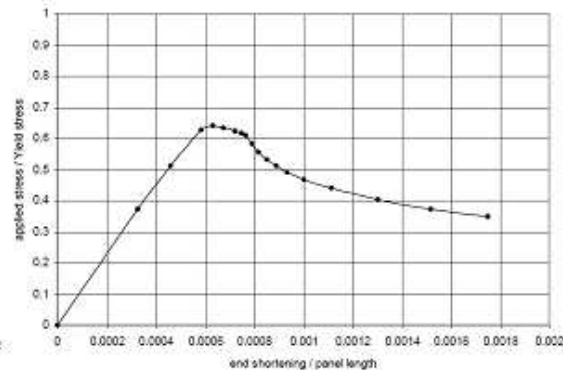


(Figure 8): Curve of changes of ( $\frac{\delta_{end}}{\delta_{int}} - \frac{\sigma_{uF}}{\sigma_y}$ ) of MRI sample

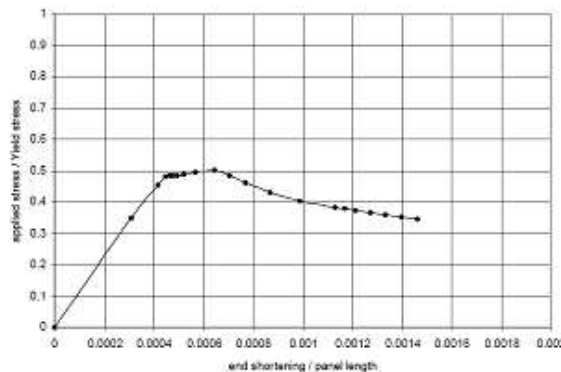


(Figure 9): Curve of changes of ( $\frac{\delta_{end}}{\delta_{int}} - \frac{\sigma_{uF}}{\sigma_y}$ ) of ML1 sample

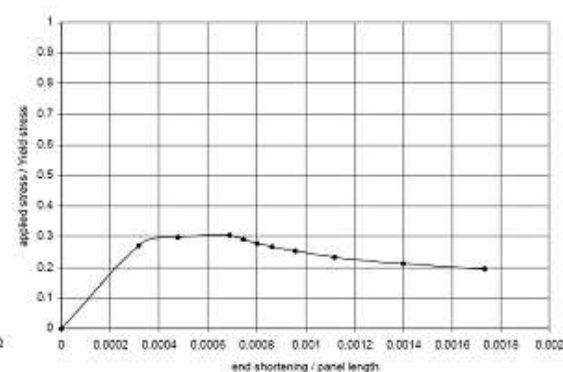


(Figure 10): Curve of changes of ( $\frac{\delta_{end}}{\delta_{int}} - \frac{\sigma_{uF}}{\sigma_y}$ ) of MT1 sample

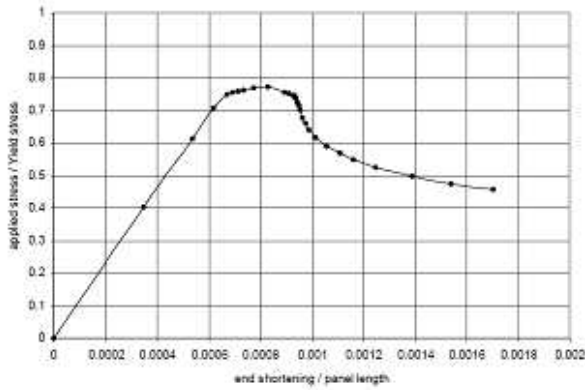


(Figure 11): Curve of changes of  $(\frac{\sigma_{max}}{\sigma_{max}} - \frac{\sigma_{min}}{\sigma_{min}})$  of MR2 sample

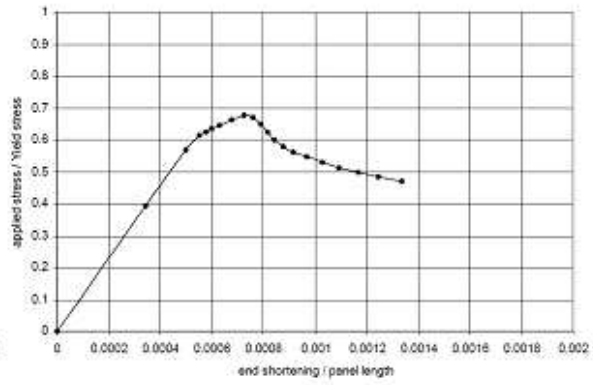


(Figure 12): Curve of changes of  $(\frac{\sigma_{max}}{\sigma_{max}} - \frac{\sigma_{min}}{\sigma_{min}})$  of ML3 sample

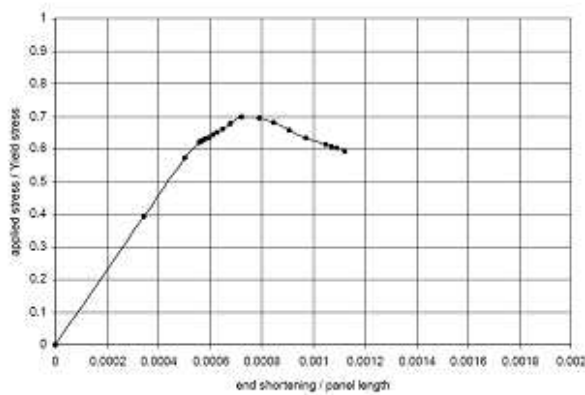


(Figure 13): Curve of changes of  $(\frac{\sigma_{max}}{\sigma_{max}} - \frac{\sigma_{min}}{\sigma_{min}})$  of MT2 sample

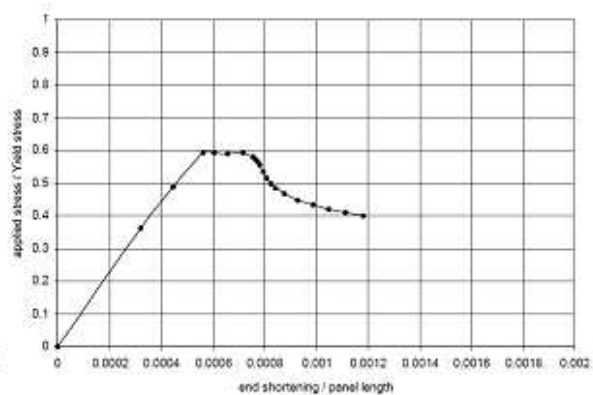


(Figure 14): Curve of changes of  $(\frac{\sigma_{max}}{\sigma_{max}} - \frac{\sigma_{min}}{\sigma_{min}})$  of MR3 sample

Comparing the results shows that in general status, there is a concurrency between the FEM results and lab results. The highest difference of samples is between 0.046 and 0.042 for samples of lines 12 and 9; respectively, of Ghosh tests. The two maximum values are for plates with L shape stiffeners that do not have geometric symmetry. In general status, simplifying the initial geometric imperfection in the FEM simulation group shows that intrinsic difference (this simplification includes the welding residue stresses and initial deformations) in the tests and lack of full continuity of simple supports in both complexes caused more incompatibility and should be carefully considered. The FEM simulation results for the lab samples of Ghosh show that fracture takes place following local buckling instability of sheet panels and this good prediction has been made by FEM for the stiffened model as explained with 6 percent difference only in the MR2 model and in other models, the difference between the numerical results and lab results is higher.

**The impacts of cross section and number of stiffener**

The impact of cross section and the number of stiffeners have been explained in the numerical analysis with the curve including dimensionless parameters of the stress imposed to the submission stress of sample materials with dimensionless parameters of deformation of end part of sample to the initial length of sample in numerical analysis. Figures (7-22) presents the curves related to the samples.



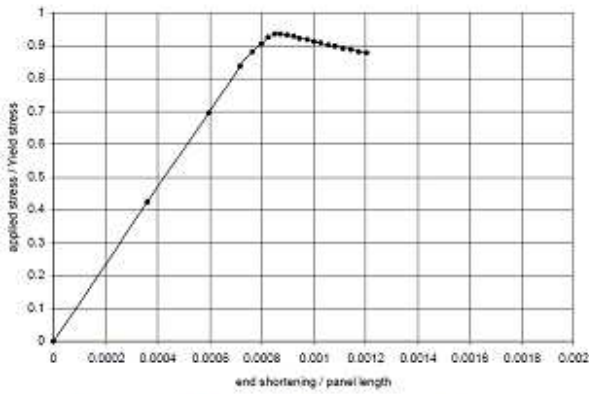


(Figure 16): Curve of changes of  $(\frac{\delta_{end}}{\delta_{it}} \frac{\sigma_{uF}}{\sigma_y})$  of MT3 sample-

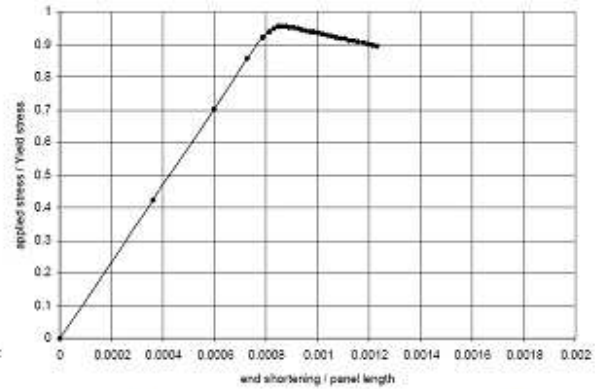


(Figure 15): Curve of changes of  $(\frac{\delta_{end}}{\delta_{it}} \frac{\sigma_{uF}}{\sigma_y})$  of ML3 sample

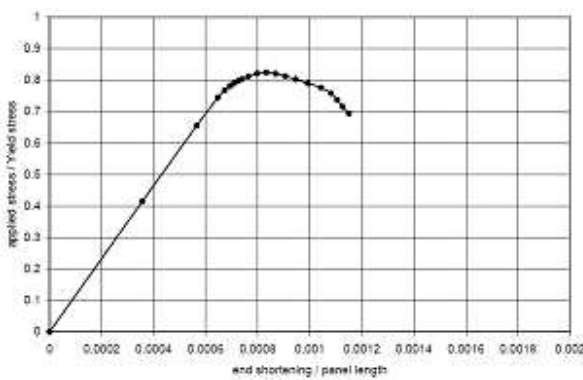


(Figure 17): Curve of changes of  $(\frac{\delta_{end}}{\delta_{it}} \frac{\sigma_{uF}}{\sigma_y})$  of MR4 sample-

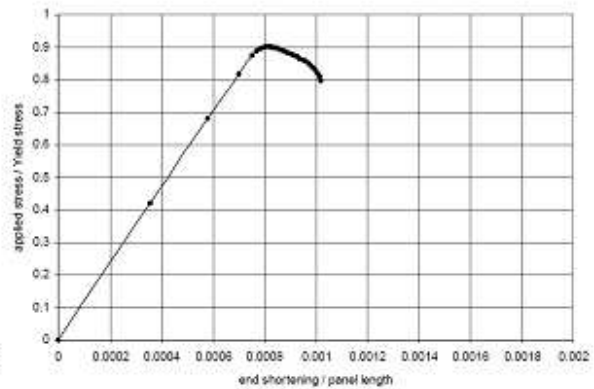


(Figure 18): Curve of changes of  $(\frac{\delta_{end}}{\delta_{it}} \frac{\sigma_{uF}}{\sigma_y})$  of ML4 sample

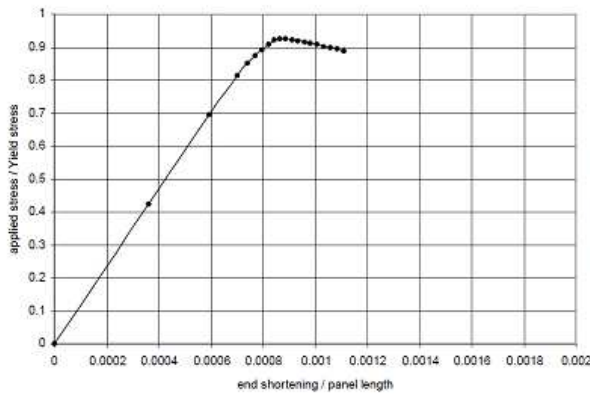


(Figure 19): Curve of changes of  $(\frac{\delta_{end}}{\delta_{it}} \frac{\sigma_{uF}}{\sigma_y})$  of MT4 sample

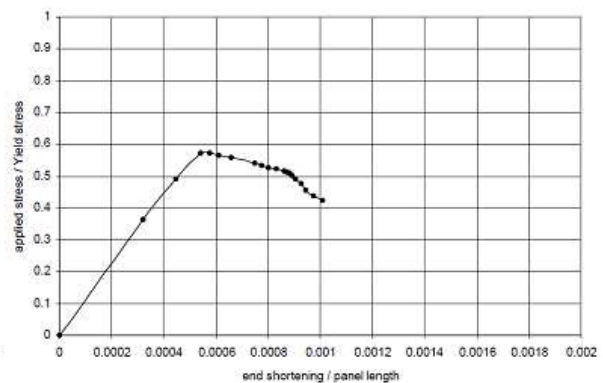


(Figure 20): Curve of changes of  $(\frac{\delta_{end}}{\delta_{it}} \frac{\sigma_{uF}}{\sigma_y})$  of MR5 sample-

Described as, with T shape stiffening, the model has the least longitudinal deformation and with R shape stiffener, the model has the highest longitudinal deformation. The stiffening work in models started from (...) = 0.00098 and reached to (...) 0.0019. The final resistance of buckling in models started from 40 percent of submission resistance and increases to 70 percent in samples. The results of FEM shows around 5 percent difference with lab results, mostly related to the deformation and initial welding. By imposing pressure force in length direction of the internal frame opening deforms with an ascending or descending sinus half wave that the priority of deformation of stiffened sheet is first, by plate buckling mode and then, the buckling mode of stiffeners. Some examples of the deformations are shown in pictures (23 and 24).

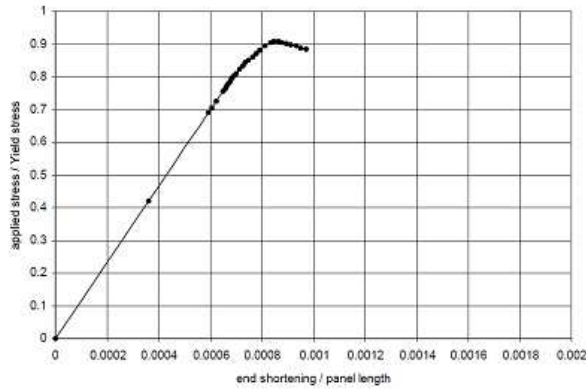


(Figure 21): Curve of changes of  $(\frac{\delta_{end}}{\delta_{it}} \frac{\sigma_{uF}}{\sigma_y})$  of ML5sample

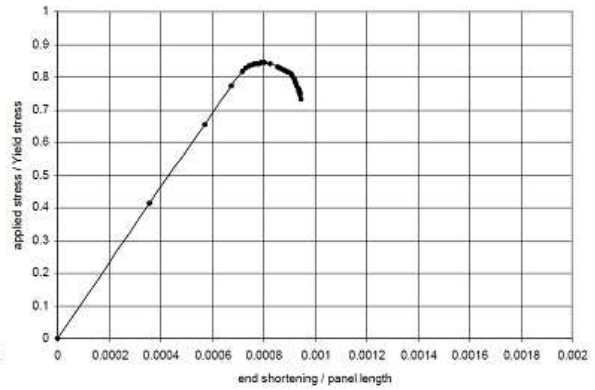


(Figure 22): Curve of changes of  $(\frac{\delta_{end}}{\delta_{it}} \frac{\sigma_{uF}}{\sigma_y})$  of MT5sample -

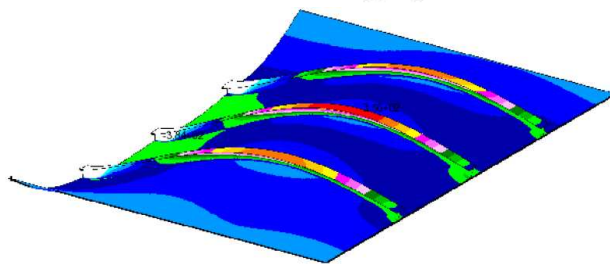


(Figure 23): Deformation caused by imposing axial load in MT3 sample

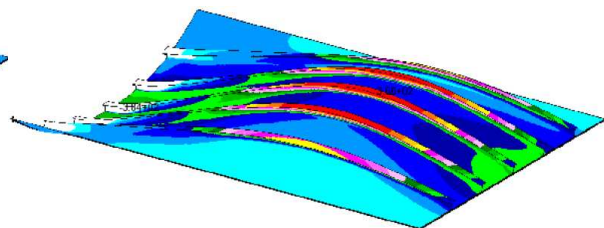


(Figure 24): Deformation caused by imposing axial load in MT5 sample

The initial conventional deformations with the same ascending and descending sinus semi-waves along with destruction of an opening push a structure towards full destruction. The local and general buckling modes have been presented as critical buckling stress values. The necessary rotation clamps have been provided by stiffeners on time of local buckling of the plate. In addition, the buckling possibility of stiffeners has become limited because according to the hypotheses, while the plate does not buckle, the stiffeners will remain sound and proper. If the web stiffeners are thin (regardless of tall and thin), the web stiffeners will buckle and the stiffeners could not provide the full theoretical rotation clamping in their path. Figure (25) shows this type of destruction.

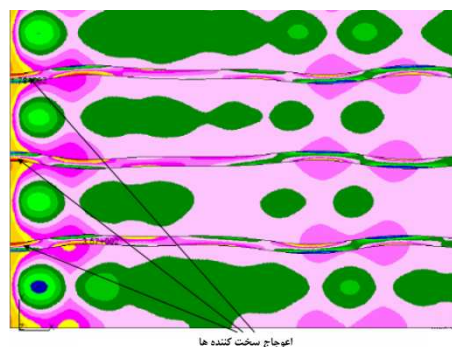


(Figure 25) :Distortion of thin stiffeners in sample MR3

## RESULTS

1. This research proved the ability of the innovated numerical method in analyzing the non-linear buckling of stiffened plates with high simulation precision of lab samples.
2. Some simplifications in simulation of the initial geometric imperfection and welding residue stress cause increase in speed and decrease in values of calculation.
3. Plastic deformations cause local buckling in plate.
4. Final rupture of samples is caused by buckling of plate and the buckling of length stiffeners mounted on it.
5. For non-elastic analysis modeling of plates, all mechanisms that lead to structure destruction should be employed.
6. Precision in fracture load as obtained in FEM simulation method showed good conformity with lab results.



7. In conditions when border conditions of simple supports were not full, large differences were seen in the numerical results and Ghosh lab results.

8. Prediction of local buckling resistance value of stiffened sheets has been made with good precision.

#### REFERENCES

- [1] G.J.Hancock. *Thin- Walled Structures.*, **1997** (1): 3-12.
- [2] Y. Chen. *Virginia Polytechnic Institute and State University, Blacksburg, VA, January.* **2003**.
- [3] F. Bleich. Bucking strength of metal structures, *McGraw-Hill, New York.* **1952**.
- [4] Karlsson, I. Sorensen. *ABAQUS ABAQUS/Standard user's manual.*, **2002**. Vol.I-III, ver.6.1, Hibbitt.
- [5] M. Pala. *Journal of Constructional Steel Research.*, **2006**. 62:716-22.
- [6] B. Ghosh. Consequences of Simultaneous Local and Overall Buckling in Stiffened Panels, PhD. **2003**.
- [7] R. Schardt. *Thin-Walled Structures.*, **1994**. 161-80.